Journal of Engineering Physics and Thermophysics, Vol. 84, No. 6, November, 2011

SOLUTION OF THE COUPLED THERMOMECHANICAL PROBLEM OF HYDRODYNAMICS FOR DESIGNING THE PROPULSION SYSTEM OF MICROSATELLITES

I. A. Miklashevich, E. A. Belogurov, and Ya. I. Shukevich

UDC 629.7.036:621.45

This paper considers the problem of predicting the technical and operating characteristics of the propulsion system of a microsatellite created by microelectronic technology. The coupled thermomechanical problem of hydrodynamics has been solved by the ANSYS CFX package. The microengine design has been optimized, the heating of its case in the operating time of the fuel chamber has been analyzed, and the velocity field distribution in the microengine nozzle has been determined. The values of the mechanical and temperature deformation fields for pure silicon and a silicon–SiO_2 composite have been found, and the possibility in principle of operation of the considered device has been shown. The calculation was made on a triangular net.

Keywords: *numerical calculation, gas flow, microengine, jet nozzle.*

Introduction. The universal finite-element gas-dynamic package ANSYS CFX offers developers flexible and effective algorithms for numerical simulation of gas-dynamic and thermophysical processes. This is largely due to the fact that the application of nonstructured finite-element meshes makes it possible to consider the gas dynamics and the heat exchange in multidimensional regions of arbitrary geometry. The above package can also be used to calculate the aerogasdynamics of jet nozzles that is an integral part of the gas dynamics of flows in channels, the theory of aircraft and rocket engines, and the aerodynamics of flying vehicles [1].

It should be noted that the gas flow in jet nozzles in the general case is rather complex (three-dimensional, pulsating, turbulent, with a high temperature, with shocks, with possible detached zones, etc.). For such a flow the basic equations of motion can only be solved numerically, which requires considerable expenditures of time and large RAM capacities of the work station or a cluster. In most cases, this leads to the necessity of using simplified or idealized flow schemes (models) facilitating the description of the gas flow and numerical calculations. In so doing, it is very important to see or determine how adequately these models reflect the real processes in the gas flow, for example, in jet nozzles, and their application in each considered case requires a special thorough analysis and experimental confirmation. Comparison between the calculated and experimental data has shown that in many cases even simple flow models make it possible to adequately describe, in general, the phenomena taking place in jet nozzles [2].

Formulation of the Problem. We consider the temperature fields and the stressed-strained state of an assembly of miniature jet nozles made from silicon by the MST technology. The assembly represents a modular construction consisting of identical jet nozzles. The number of elements (separate emgines) in the assembly may vary depending on the technical assignment. Each element is technologically assembled from two identical halves. The computational domain represents a channel of prismatic form with various abrupt junctions, including also junctions with sudden shrinkage. The given form reflects the features of the production process and is far from being ideal in terms of the gas dynamics.

Figure 1 shows the geometrical shape of the microengine nozzle. Mechanically, the nozzle is made from two identical parts joined on the horizontal surface by special methods into a single part. The nozzle length is 50 mm, the width is 4 mm, and the length of the cylindrical part is 15 mm. The finite-element discretization was carried out by tetrahedrons, the total number of elements was taken to be equal to 4 million, and the size of the tetrahedron side was about $2 \cdot 10^{-5}$ m. A test calculation for 6 million elements was carried out. The obtained results differed insignificantly, which enables us to take the number of finite elements equal to 4 million to be optimal for our problem, since the

Belarusian National State University, 65 Nezavisimost' Ave., Minsk, 220013, Belarus; email: miklashevich@yahoo.com. Translated from Inzhenerno-Fizicheskii Zhurnal, Vol. 84, No. 6, pp. 1239–1245, November–December, 2011. Original article submitted December 29, 2010; revision submitted June 23, 2011.

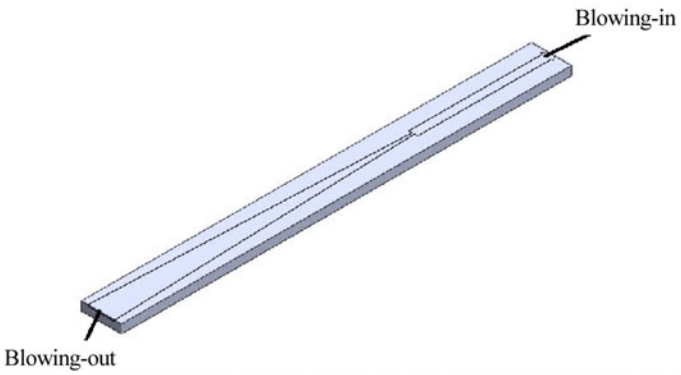

Fig. 1. Geometrical shape of the microengine nozzle (section on the joint surface).

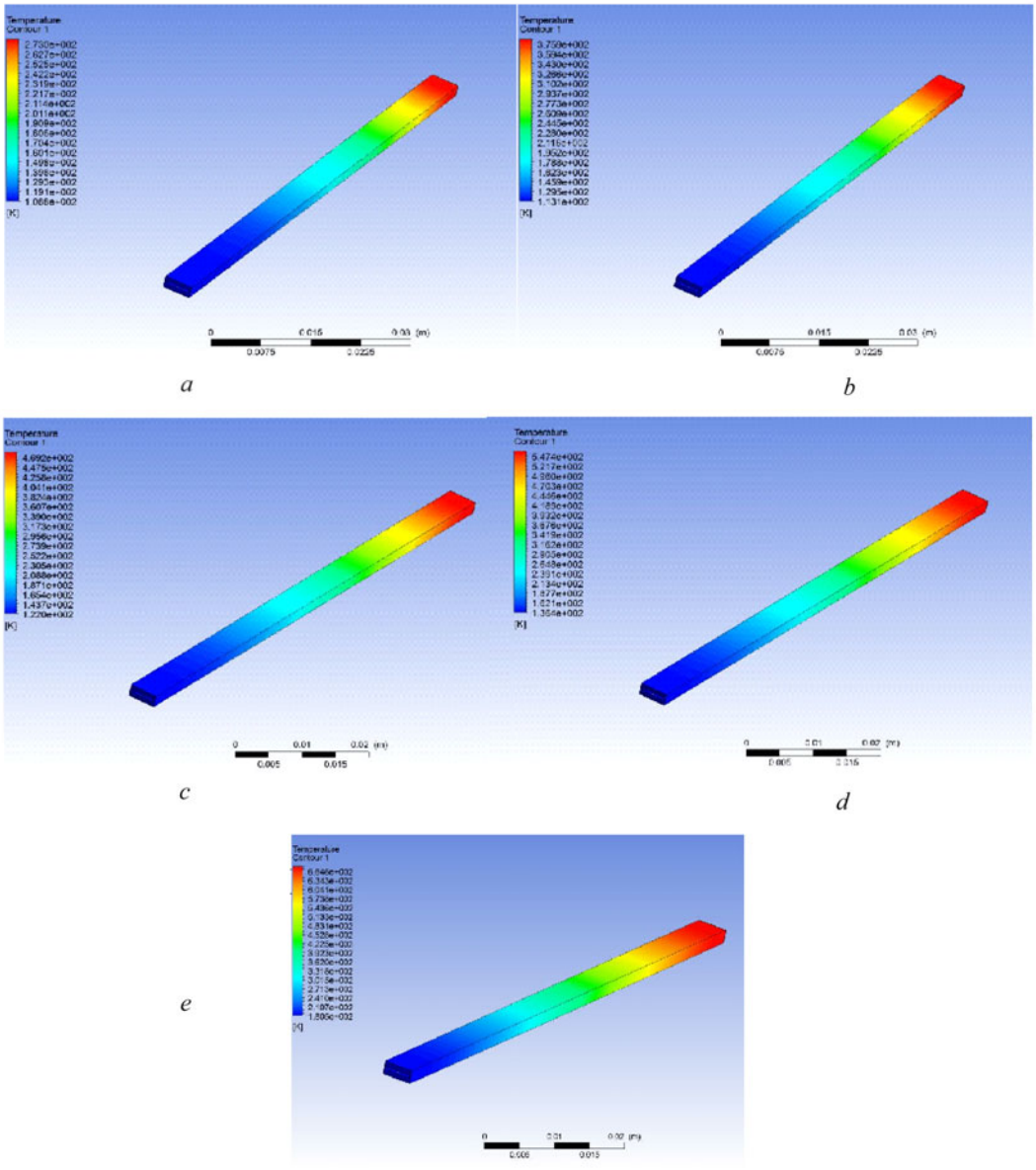

Fig. 2. Temperature distribution over the surface of the microengine case depending on the time of gas passage through it: a) 1 s; b) 2; c) 3; d) 4; e) 5.

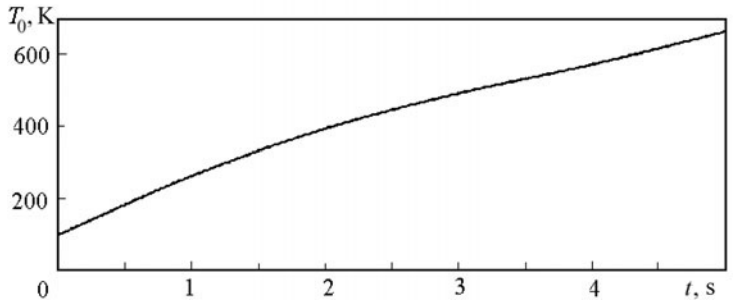

Fig. 3. Time dependence of the heating of the microengine case.

use of finer meshes makes no appreciable contribution to the accuracy of results but leads to a considerable increase in the calculation time.

We solved the problem of determining the time dependence of the temperature field of the microengine case (one element of the propulsion system of the microsatellite) and the gas velocity field along the length of its nozzle. This process is described by the standard energy balance equation and the equation of heat transfer with the environment:

$$\frac{\partial (\rho h_{\text{tot}})}{\partial t} - \frac{\partial \rho}{\partial t} + \nabla (\rho U h_{\text{tot}}) = \nabla (\lambda \nabla T) + \nabla (U\tau) + US_{\text{im}} + S_{\text{h}} , \tag{1}$$

$$-\mathbf{n}(-\lambda \nabla T_{\text{b}}) = q_0 + h (T_{\text{out}} - T_{\text{b}}) + \varepsilon\sigma (T_{\text{amb}}^4 - T_{\text{b}}^4) , \tag{2}$$

where h_{tot} is the total enthalpy related to the static enthalpy $h(T, p)$ by the relation $h_{\text{tot}} = h + 1/2U^2$. The term US_{im} describing the external impulse work is neglected in the existing realizations of the program product.

To simplify the problem, the heat transfer into the environment (body of adjoining elements of the assembly) was simulated with the use of a heat transfer coefficient at the boundary equal to 10 W/(m^2·K), and the radiative heat exchange was taken into account by introducing an emissivity equal to 0.7. The intrinsic viscosity of the gas was determined by a coefficient equal to $18.8 \cdot 10^{-6}$ Pa·s. The obtained temperature distributions on the microengine case as a function of time are given in Fig. 2.

Figure 3 shows the time dependence of the maximum temperature of the microengine case. As is seen from this graph, the microengine case is heated uniformly throughout the time of its operation.

The gas flow turbulence in the nozzle was determined with the use of the standard k–ε model. This model includes two transport differential equations for calculating the kinetic energy k and the turbulent dissociation ε. It permits obtaining stable results, does not require considerable computational resources, and has been used for a long time as an industrial standard. The above model proved to be effective in calculating internal flows but presents problems in calculating flows with large pressure gradients and separation and gives the beginning of separation with a large delay and underestimated sizes of detached flows [3].

The application of the k–ε model presupposes the solution of two additional equations for the turbulent kinetic energy and dissipation rate:

$$\frac{\partial (\rho k)}{\partial t} + \nabla (\rho U k) = \nabla \left[\left(\mu + \frac{\mu_{\text{t}}}{\sigma_{\text{k}}} \right) \nabla k \right] + P_{\text{k}} - \rho\varepsilon , \tag{3}$$

$$\frac{\partial (\rho\varepsilon)}{\partial t} + \nabla (\rho U \varepsilon) = \nabla \left[\left(\mu + \frac{\mu_{\text{t}}}{\sigma_{\varepsilon}} \right) \nabla \varepsilon \right] + P_{\text{k}} - \frac{\varepsilon}{k} (c_{\varepsilon 1} P_{\text{k}} - C_{\varepsilon 2} \rho\varepsilon) . \tag{4}$$

Here the generation of dissolution [3] consists of three terms, the first two of which define the generation of dissipation due to the turbulent mixing in the averaged motion, and the last term in the pulsation motion. The term ρε is called dissipative and defines the dissipation of turbulence dissipation [3].

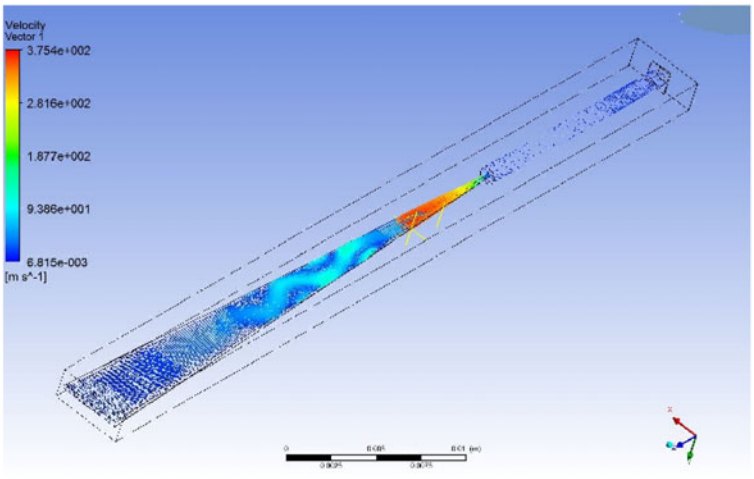

Fig. 4. Distribution of the gas velocity field in the nozzle.

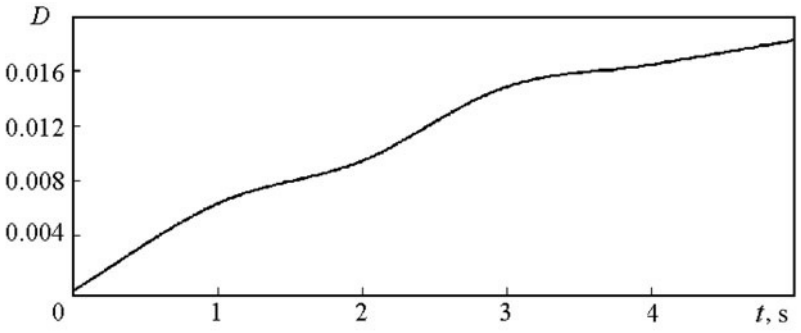

Fig. 5. Time dependence of the mechanical deformation of the microengine case.

Strictly speaking, all terms on the right-hand side of Eqs. (3) and (4) require special modeling, since the system of these equations in any combination with equations for turbulence characteristics is not closed. Such modeling can be carried out by direct numerical calculation (e.g., DNS); however, such a calculation requires considerable resources and is used in exceptional cases. Therefore, we used conventional values of parameters in solving the problem under consideration [4]. With the use of the accepted turbulence model from Eqs. (1), (2) we obtain the distribution pattern of the gas velocities along the entire nozzle of the microengine (Fig. 4).

To take into account the thermomechanical deformations and stresses arising in the construction, we solved the system of Duhamel–Neumann equations:

$$\sigma_{ij}(\mathbf{r}) = C_{ilkl}(\mathbf{r})\,\varepsilon_{kl}(\mathbf{r}) - \beta_{ij}(\mathbf{r})\,\theta(\mathbf{r}), \quad \varepsilon_{ij}(\mathbf{r}) = S_{ilkl}(\mathbf{r})\,\sigma_{kl}(\mathbf{r}) + \alpha_{ij}(\mathbf{r})\,\theta(\mathbf{r}).$$

Figure 5 shows the time dependence of thermomechanical deformations arising in the microengine case plotted with account for the temperature dependence of the elastic modulus of silicon. As is seen from the plot, the thermomechanical deformations increase practically linearly with time. This plot correlates fairly well with the plot of the microengine case heating shown in Fig. 3. Analysis of the dependences presented in Figs. 3 and 5 shows that the dominant contribution to the development of deformations of the microengine case is made by the "temperature" component.

Analysis of the Obtained Results. To solve the problem under consideration, a triangular net was used. Approximation was carried out by the Lagrange polynomial of the second kind, since the use of the third-order approximation scheme leads to a considerable nonmonotonicity of the solution. In turn, the presence of nonmonotonicity leads to a strong distortion of the flow topology [5].

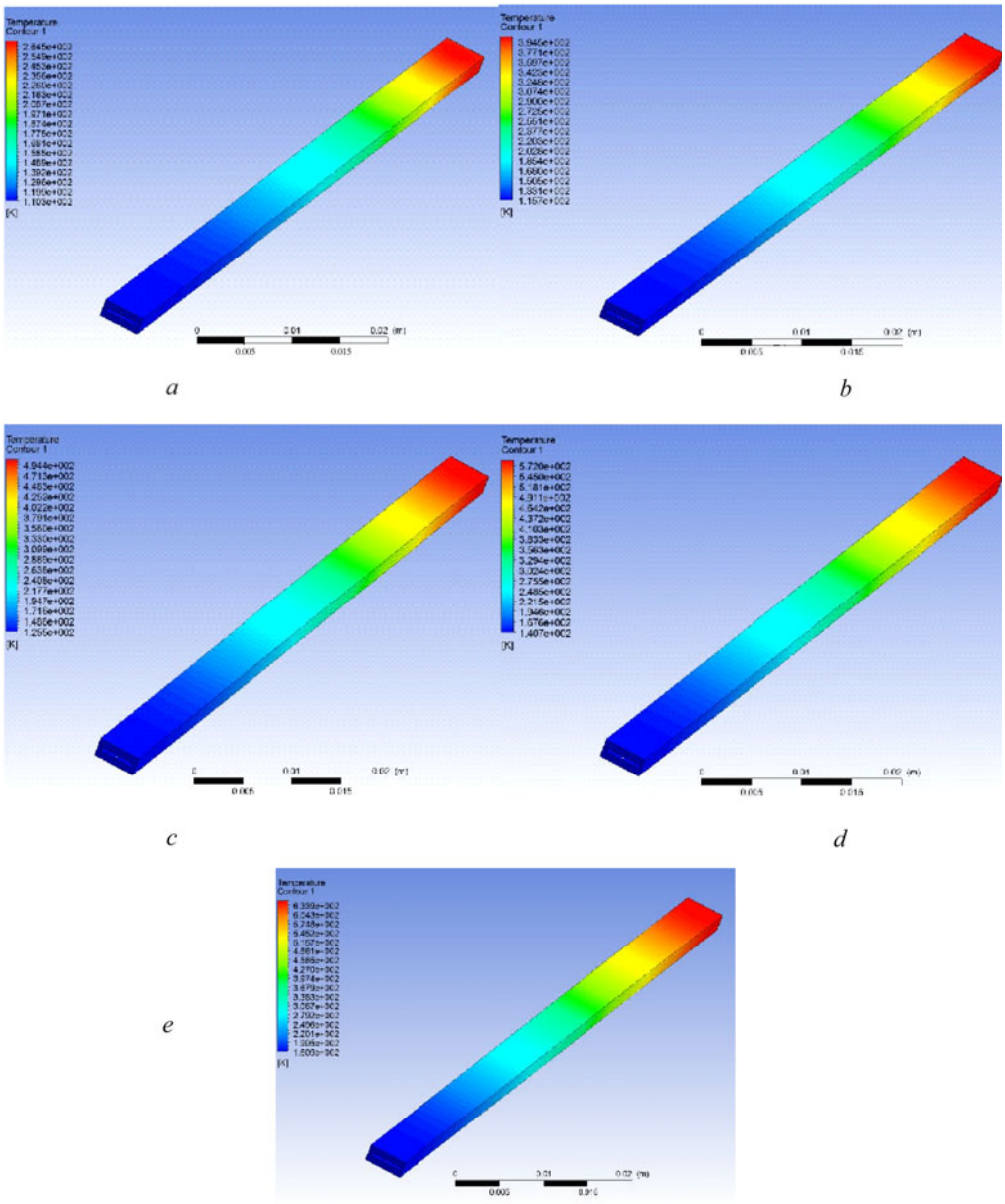

Fig. 6. Temperature distribution over the surface of the microengine case depending on the operating time of the fuel chamber: a) 1 s; b) 2; c) 3; d) 4; e) 5.

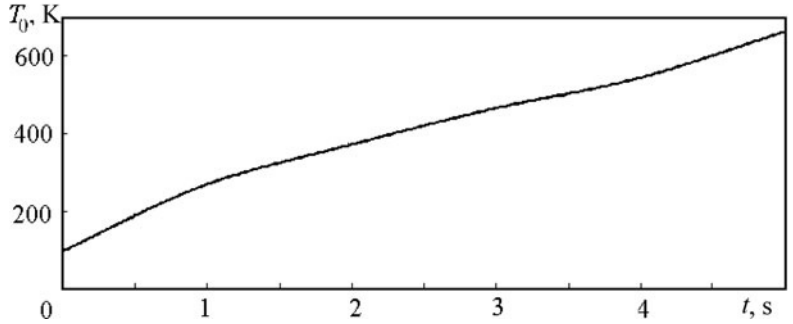

Fig. 7. Temperature of the upper surface of the microengine case versus the operating time of the fuel chamber.

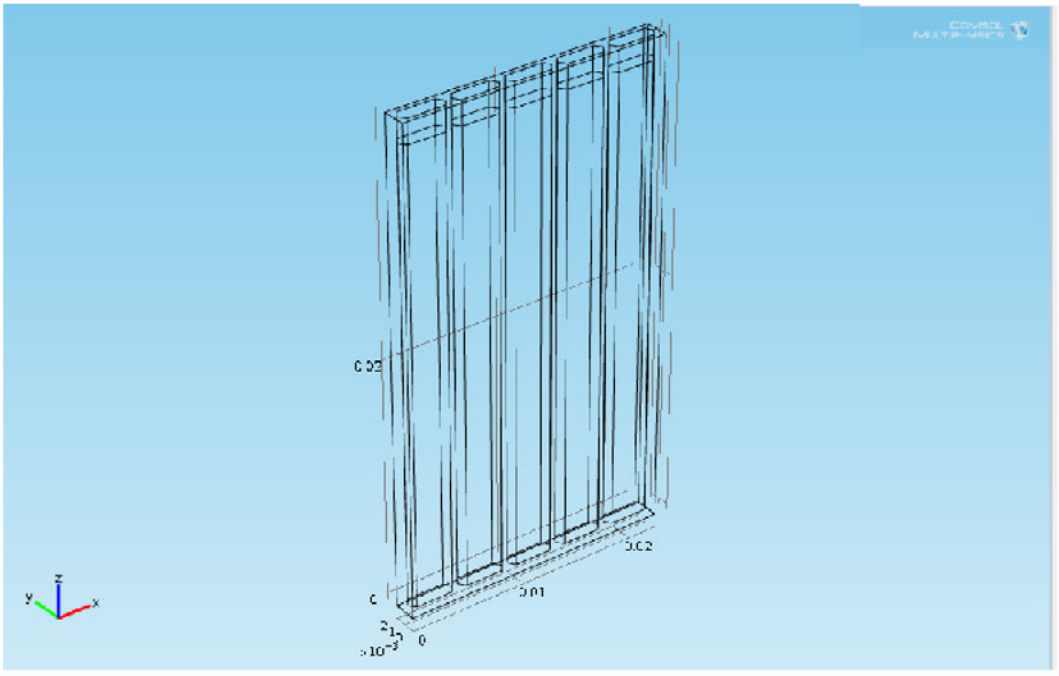

Fig. 8. Assembly from five fuel cells.

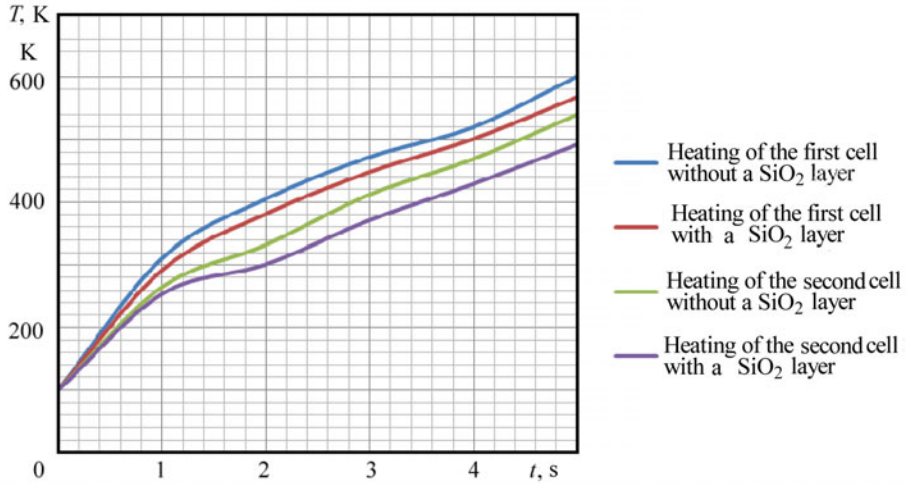

Fig. 9. Time dependence of the heating of the case of individual elements of the assembly.

For an individual cell we considered the practically ideal case where its six sides participate in the convective and radiative exchange, but since the real construction represents an assembly from 5 or 25 such cells, the radiative and convective heat exchange will only be present on the facets of the assembly. Therefore, strong heating of the central cell that can lead to the fuel ignition in the adjoining cells is possible. To assess the possibility of preventing it, we decided to introduce a SiO_2 barrier layer [6] of thickness 1 μm. This thickness was chosen with account for the technological features of the SiO_2 film formation. The results obtained for such a microengine are shown in Figs. 6, 7. As is seen from the plot presented in Fig. 7, the introduction of the SiO_2 barrier layer for a single cells does not lead to an appreciable change in the temperature field distribution over the case surface. The influence of the SiO_2 layer for an assembly of five cells (Fig. 8) is shown in Fig. 9. The need for a separate analysis of the assembly of cells is due to the possible influence of the working cell on the state of the neighboring cells. As follows from Fig. 9, in the presence of a SiO_2-layer the heating of the neighboring cells is weaker when the fuel cell operates for a time longer than

1.5 s. The introduction of the barrier layer can be of practical importance in developing an assembly of 25 cells when radiative and convective heat exchange is only possible for the facets of extreme cells.

Conclusions. With the aid of the ANSYS CFX finite-element package, the coupled thermomechanical problem of determining the stressed-strained state and temperature fields for a propulsion system made by silicon technology has been considered. With account for the k–ε turbulence model, the gas velocity field along the full length of the microengine nozzle has been found.

Analysis of the thermomechanical deformations arising in the microengine case has shown that its structural integrity is not affected in the process of operation and the product is functionally serviceable. Local regions of overstresses in a real structure that are due to heating can relax and do not lead to a failure of the cell. Taking into account the operation of not one cell but of a matrix of 25 cells, it is expedient to use a barrier layer of silicon dioxide in order to decrease the temperature of the microengine case.

This work was supported by the scientific-technical program of the Union State "Nanotechnology-SG" (assignment No. 2.2.3/BNTU). Modeling was carried out with the use of the computer equipment and software of BY-BNTU and SKIF-Grid clusters developed and created with support from the project of the EU seven-frame program "Balticgrid II," a NATO PDD(SPS) (EAP.NIG.983696), grant and the Union State program "SKIF-Grid."

NOTATION

$C_{\varepsilon 1}$, $C_{\varepsilon 2}$, turbulence constant equal to 1.44 and 1.92, respectively; C_{ijkl}, tensor of elastic moduli, N/m^2; D, thermomechanical deformations; k, kinetic energy per mass unit, m^2/s^2; **n**, normal vector; q_0, thermal flow, W/m^2; **r**, position vector; S_h, volume heat source, J/m^3; S_{im}, external impulse, kg/(m^2·s^2); S_{ijkl}, tensor of compliance moduli, N/m^2; T_{out}, temperature of the outer surface of the microengine case, K; T_b, temperature of the fuel cell body, K; T_{amb}, ambient temperature; t, time, s; U, velocity field, m/s; α, temperature expansion coefficient, 1/K; β_{ij}, thermal stress field, Pa; ε, degree of dissipation of turbulence, m^2/s^3; ε_{kl}, tensor of mechanical deformations; θ, temperature differential, K; λ, heat conductivity coefficient, W/(m·K); μ, molecular viscosity, kg/(m·s); μ_t, turbulent viscosity, kg/(m·s); ρ, gas density, kg/m^3; σ, mechanical stress, Pa; σ_{ij}, tensor of total stresses, Pa; σ_k, turbulence constant for the kinetic energy transfer equation assumed to be equal to one; $\sigma\varepsilon$, turbulence constant for the turbulence dissipation transfer equation; τ, tensor of shear stresses, Pa; ∇, Hamilton operator. Subscripts: h, heat; im, impact; out, outer; b, body; amb, ambient; k, kinetic; t, turbulent.

REFERENCES

1. G. I. Lavrukhin, *Aerodynamics of Jet Nozzles* [in Russian], Nauka–Fizmatlit (2003).
2. J. J. Connor and C. A. Brebbia, *Finite Element Techniques for Fluid Flow*, Newnes-Burterworths, London (1977).
3. I. A. Belov and S. A. Isaev, *Modeling of Turbulent Flows* [in Russian], Balt. Gos. Tekhn. Univ., St. Petersburg (2001).
4. S. A. Isaev and D. A. Lysenko, Testing of numerical methods, convective schemes, approximation algorithms for of flows, and grid structures with the example of a supersonic flow in a step-shaped channel with the use of the CFX and FLUENT packages, *Zh. Tekh. Fiz.*, **82**, No. 2, 326–330 (2009).
5. *ANSYS*, *Inc Ansys CFX Solver Theoretical Cuide*, Canonsburg (2006).
6. United States Patent, 6378292, Youngner, April 30, 2002. Appl. No. 09/709107.